International Journal of Advanced Research in Science Management and Technology
ISSN(Online)-2454-4159 Volume 3, Issue 4, April 2017

"Discrimination of Lung Cancer Cells by using Automated Near-Infrared Liquid-Crystal Polarimetric Imaging System for Discrimination of Lung Cancer Cells: A Review"

Amruta Patil[1], Prof. Mrs. J. H. Patil[2]

PG Scholar, Department of E&TC Engineering, D. N. Patel College of Engineering, Shahada, Maharashtra, India[1]

Professor, Department of E&TC Engineering, D. N. Patel College of Engineering, Shahada, Maharashtra, India[2]

Abstract— A recently created tissue demonstrative technique, in light of label-free close infrared (NIR) polarimetric reflectance imaging for the characterization of histopathological tests of lung cancer cells, is displayed. The design, calibration, and testing of an automated NIR polarimetric imaging framework, with accentuation on lung cancer location, are advanced in detail. The depicted electro-optical imaging polarimeter framework shows high level of precision and repeatability. The result of this paper shows that the operational design standards of the NIR polarimetric framework might be demonstrated to a great degree helpful in Segregation of label-free normal and lung cancer cell tests and additionally differentiation of various lung cancer cells and stages in vitro.

Keywords— Adenocarcinoma, automated near infrared (NIR) reflectance polarimeter, calibration, clinical applications, design, high specificity, Mueller matrix, NIR label-free cell differentiation, normal lung cancer cells, squamous carcinoma, testing.

I. INTRODUCTION

IN THIS paper, a recently created tissue analytic technique, in light of label-free close infrared (NIR) polarimetric reflectance imaging for the arrangement of lung cancer histopathological tests from a tissue slide, is exhibited. The design, calibration, and testing of an automated NIR polarimetric imaging framework going for creating proficient what's more, dependable symptomatic methods, with accentuation on lung cancer discovery, are exhibited, examined, and talked about according to [1], there have been an aggregate of 1.59 million passing's from lung cancer in 2012. There are basically two sorts of lung cancers, little cell lung cancer and no small-cell lung cancer (NSCLC), of which 87% are analyzed as no small cell. Most fringe tumors are adenocarcinomas or substantial cell carcinomas. On account of their fringe area, adenocarcinomas may not be gotten ahead of schedule until they have created extra thoracic metastases.

For instance, patients may appear clinical indications of bone spread or intracranial metastatic malady. Then again, squamous cell carcinoma of the focal aviation route is thought of as a multistep procedure beginning from a Squamous metaplasia, which advances to dysplasia, took after via carcinoma in situ (CIS), at long last advancing to obtrusive cancer [8].

There are various identification procedures, which could be either noninvasive or biopsy strategies, as of now utilized for early lung cancer identification. Some of them are highlighted. The basic location systems for lung cancer are traditional imaging systems like trunk radiography (film or computerized) and figured tomography (CT). Computerized radiography furnishes better balance determination with equivalent or better spatial determination when contrasted with traditional radiography procedures [2]. Notwithstanding, these systems still do not give conclusive data that can be used toward the early recognition of tumors. Low-measurement winding/helical CT can be a promising methodology for lung cancer screening. Be that as it may, it is restricted to little fringe sores. Overwhelming smokers create tumors situated in the focal aviation routes, and therefore, other methods other than CT are required for early recognition [3], [4].

International Journal of Advanced Research in Science Management and Technology
ISSN(Online)-2454-4159 Volume 3, Issue 4, April 2017

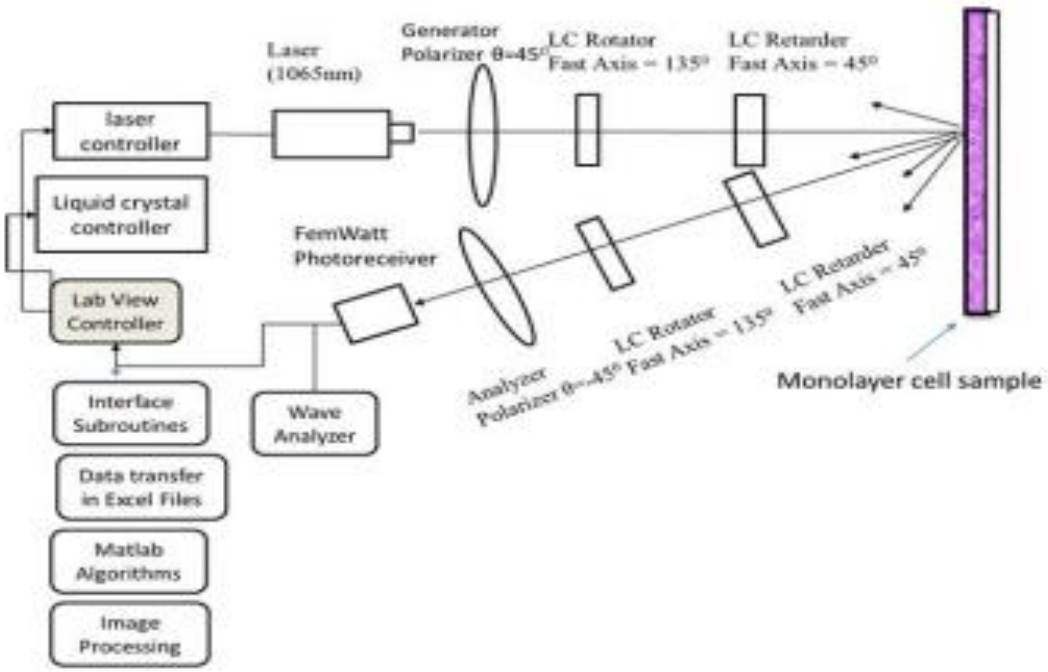

Fig.1 Air Force Research Laboratory (AFRL) polarimetric imaging platform.

Optical imaging includes testing tissue with light waves in the upper UV, obvious, NIR, and infrared districts (400–1500 nm). Concentrate the optical properties of tissue uncovers data that can possibly describe maladies [5]–[7]. It can give metabolic data consolidated with anatomical data, which upgrades the identification procedure of early cancer. White light bronchoscopy, auto fluorescence imaging, limit band imaging, high magnification bronchovideoscopy, end bronchial ultrasound, furthermore, optical soundness tomography are the at present utilized optical imaging systems that have been produced to upgrade the capacity to analyze NSCLC at a pervasive organize.

II.LITERATURE SURVEY

Truly, numerous striking advances of optical polarimetry have been created for remote detecting and biomedical applications. Baba et al. [14] built up an automated polarimetric stage, utilizing fluid gem (LC) optical parts. The calibration of that framework was tried against tests with known Mueller grids like air also, direct polarizers. Afterward, the framework was changed by Baldwin et al. [15] to play out the Mueller matrix imaging for skin cancer recognition utilizing a 14-bit charge-coupled gadget (CCD) camera as an identifier. The normalized force of each of the Mueller matrix components demonstrated huge contrasts amongst cancerous and noncancerous tissues. Rovati et al. [16] built up a polarimetric framework utilizing two He–Ne lasers and an exact simple stage to-voltage converter. The execution of the framework was checked utilizing diverse glucose tests of known fixation. The framework could quantify the grouping of bianisotropic particles in arrangements.

Liu et al. [17] built up another framework that used LC gadgets, LabVIEW, PC control, and CCD imager. In this paper, the value of polarimetry was exhibited by separating subtle elements not seen by nonpolarization-delicate imaging. The depicted framework comprised of an example, a generator, and an analyzer, which were altogether settled with 45° between the generator and analyzer, however the question revolution was not considered. Giakos [18] exhibited picture improvement that used a mix of both multispectral imaging and the level of straight polarization (DOLP) to upgrade a solitary picture. Hooper et al. [19] built up an airborne imaging framework comprising of numerous cameras that could take pictures remotely in a few otherworldly groups alongside three isolated polarization states. This strategy did not use full polarimetric estimations; in any case, DOLP pictures were appeared to highlight the components of geographical enthusiasm with more noteworthy specificity. Another polarimetric stage was produced by Bueno [20],

which likewise used LC optical segments for framework calibration that required manual inclusion of the optical segments. Buscemi et al. [21] built up another polarimetric imaging system that empowered continuous multispectral securing of level of polarization (DOP) with applications to biomedical applications. The polarimetric framework created acquired the DOP as an element of stage and polarization of the episode shaft considering the variety of only one parameter in the setup.

A portion of the polarization sensors have likewise been presented by various gatherings for various applications. Zhao et al. [22] presented a polarization heading sensor in light of a novel point calculation. The sensor was produced with three heading analyzers, with the polarization tomahawks of the positive channel acclimated to 60° to each other. This sensor acknowledged high-exactness route with photoelectric material copying the capacity of the compound eye of abandon ants.

Morawski et al. [23] presented a calibration method of spectrophotometric transducers. Different semisynthetic reference information, gotten by numerical change, were utilized for the investigation of the calibration method. This calibration strategy appeared to be imperative for applications with various sorts of spectroscopy with energized light. In [24], an infrared laser light-based scanner was introduced to get the state of nonopaque protests by concentrate the conduct of the materials outside the noticeable range. The study was performed by gaining the warmth designs discharged by the question. Correspondingly, Sarkar et al. [25] built up a CMOS picture sensor for the discovery of approaching light beams utilizing polarization data. It was demonstrated that the polarimetric data like DOP, electric field vector forces and some Stokes parameters like ellipticity and azimuthal point can be utilized as a kind of perspective hotspot for route with nearly nothing many-sided quality.

III. PROPOSED SOLUTION

The imaging polarimetric framework comprises of two arms, as appeared in Fig. 1. The generator arm and the analyzer arm comprise of four polarization states: 1) even (H); 2) vertical (V); 3) +45° (P); and 4) right round polarization (RCP). Subsequently, it gives a blend of 16 estimation states, driving hence to full 16 forces of the specimen. The separation between the laser source and the test s 124.46 cm, while the separation between the specimen What's more, the photo detector is 118.22 cm. The edge between the generator and the analyzer arm is under 5°.

Light heartbeats created by a 1065-nm Picosecond Injection Laser diode framework, working at a heartbeat reiteration rate (PRR) of 200 Hz, are sent through the polarization producing branch (transmitting side), comprising of a generator polarizer set at +45°, a LC rotator, and a LC retarder, so that the directly enraptured waves keep up their underlying polarization state. The light is engaged onto the example, and the backscattered light is then recognized, in the wake of going through the analyzer arm (collector arm) subtended at 5° concerning the heading normal to the cell test. Specifically, the analyzer arm comprises of a LC retarder with the quick pivot at 45° coupled to a LC rotator with the quick hub at 135°, and an analyzer-polarizer at −45°, which are set before a 2151 New Focus 1-mm breadth silicon p-i-n diode femtowatt photodetector. The photodetector shows a phantom range between 300 and 1100 nm. The photodetector shows a ultralow clamor identical power ≤15 fW/Hz1/2, a most extreme change pick up of 1 × 1011, and an average responsivity of 0.5 A/W.

To accomplish mechanization of the framework, all the four LC parts and the femtowatt photodetector are controlled by methods for a LabVIEW created GUI, as portrayed in Section IV. The program gives the calibration voltages to the LC parts for the four polarization states, in particular, level, vertical, +45°, and RCP. The polarimetric

state powers are distinguished by the photoreceiver, and after that sent to the PC through a NI#9215 information procurement (DAQ) unit with a testing recurrence of 100 kHz. At last, they are handled utilizing Excel and MATLAB ubroutines. Six arrangements of estimations are procured, for expanded factual exactness, and afterward found the middle value of.

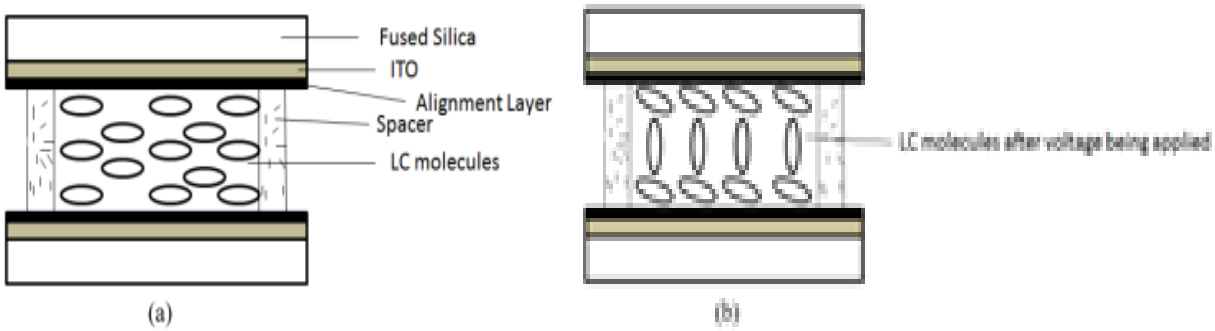

Fig.2 Operational principles of LC devices. (a) Maximum retardance (V = 0). (b) Minimum retardance (V 0).

IV. AUTOMATION OF THE SYSTEM

The mechanization of the electro-optical polarimetric imaging framework is accomplished by methods for LabVIEW and MATLAB subroutines. Therefore of this computerization procedure, the DAQ also, preparing time are significantly diminished. A graphical UI unit is produced in LabVIEW so that the calibration voltages of the LC retarders and rotators could be connected to the framework and the estimation voltage from the indicator could be perused in Excel sheets.

The information parameters that must be doled out to the framework are as per the following.

1) LC retarders and rotators calibration voltages.

2) Sampling rate for the DAQ unit utilized.

3) LC gadget postpone time.

4) Measurement Time: This is the time required for the estimation and must be more noteworthy than the defer time in addition the time required to get every one of the specimens.

5) Voltage Threshold Level: This the predetermined level of the voltage so that lone the voltage over this limit esteem is recorded, i.e., the crest to-top an incentive underneath this

level is disposed of.

6) Waveform Data: This is the quantity of information focuses gathered so that the waveform can be shown in either MATLAB or in Excel.

7) State Data: This is the base number of tests the A/D will gather, which is additionally the base number of information focuses over the limit and is given by

$$D_{\min} = \left(0.1 \times \frac{1}{F_{\text{mod}}}\right) \times \frac{1}{T_s}$$

Where Fmod is the adjustment recurrence of the laser, Ts is the inspecting time, and 10% (0.1) alludes to the obligation cycle of the laser. The yields that are acquired from the automated framework are as per the following.

1) The normal top to-crest voltages for each of the 16 states are gotten in the Excel sheet. Furthermore to this, the normal op to-crest voltage is gotten for the quantity of times the trial is rehashed in the same Excel sheet.

2) The crude crest to-top abundancy is acquired for each of the 16 states (2500 information focuses) with the goal that it could be prepared in Excel or in MATLAB.

3) Also the waveform tests are acquired for each of the states.

The nitty gritty rundown of the robotization of the framework with the information sources and yields acquired from it is appeared. The postpones utilized as a part of the framework for one specific estimation state (generator–analyzer blend) as depicted in the sources of info allocated to the framework are as per the following.

1) T0: Apply voltages to LC gadgets to control polarization states.

2) T1: Delay worked into permit adjustment of LCs. The least time is around 15 ms and is constrained by the LC gadget detail.

3) T2: Measurement time can be modified to test more information and normal more outcomes (client characterized comes about used 750 ms).

4) T3: Delay time before the following estimation.

In our framework, T 3 is been roughly 750 ms; in any case, it can be 0 if the most extreme speed is wanted. After the Excel sheets are acquired from the LabVIEW automated framework, they fill in as a contribution to the MATLAB routine to acquire the Mueller matrix of the protest under test. The MATLAB routine yields are sustained into an Excel sheet that shows the Mueller matrix of the question. A rearranged piece chart (flowchart) of the mechanization programming schedule is appeared in Fig.3.

Fig.3 Simplified block diagram of the automation software routine

V. RESULT ANALYSIS

The calibration voltages have been tried utilizing polarization channels of the known Mueller matrix, for example, a direct level polarizer (LHP), i.e., a polarizer having its transmission pivot in the level course and a straight vertical polarizer (LVP), i.e., a polarizer having its transmission hub in the vertical course. These test examinations are done in transmission mode, i.e., putting the generator and the analyzer arm in the up close and personal course. Between the generator and the analyzer arm, the test-protest is set. The polarizer (direct flat and vertical) utilized for the analysis is operational inside a wavelength scope of 700–1100 nm. Just four of the states H, V, P, and RCP were utilized for the analysis both on the generator and the analyzer arms, along these lines totaling the number of estimation states to 16 (blend of four states in the generator and analyzer arm). The test setup for the trial of the aligned information is appeared

in Fig. The hypothetical (perfect) Mueller matrix of the segments furthermore, those gotten from the trials are appeared in Table . The factual examination was performed for the Mueller matrix count of LHP and LVP to see the precision of the estimations. Likewise the plots for the perfect and Fig. Trial setup for the trial of the calibration voltages. test Mueller matrix components for air, LHP, and LVP are appeared in Figs. 16 and 17. From the factual examination, it can be watched that the standard deviations for Mueller matrix of LHP and LVP acquired are 0.0478 and 0.0364, separately. In this manner, these outcomes exhibit high level of precision of the adjusted outcomes as contrasted and the frameworks in [7] and [33] (which have the standard deviations for Mueller matrix of LHP and LVP as 0.117 and 0.0457, separately).

The numbers acquired from the framework depicted here are superior to anything ones acquired from [7] and [33]. In examination with [7], [14], and [19], the framework created in this paper is an automated one. The past improvements required manual inclusion of the optical segments or manual taking care of for DAQ. In our framework, the examinations are done in automated mode, and a similar examination can be rehashed the same number of times as required to see the reproducibility of the outcomes. Subsequent to playing out the calibration of the polarimetric framework furthermore, confirmation of the calibration systems utilizing polarization channels of the known Mueller matrix, the examinations for the solid lung cells and cancer cells were performed utilizing the test design utilizing Fig. 1, as depicted in Section II, in backscattered mode.

VI. CONCLUSION

In this paper, a recently created tissue indicative strategy, in view of label-free NIR polarimetric reflectance imaging for the grouping of lung cancer cell histopathological tests, is exhibited. The design, calibration, and testing of an automated polarimetric imaging framework going for creating productive and solid symptomatic systems, with accentuation on lung cancer discovery, were exhibited. The exhibited electro-optical imaging polarimeter framework has high level of exactness and repeatability. The framework can either be utilized for the estimation of Mueller matrix components for the example utilizing a photodetector or CCD or CMOS cameras. The segregation capability of optical polarimetric This article has been acknowledged for incorporation in a future issue of this diary. Substance is last as exhibited, except for pagination. framework was tried against label-free monolayer lung cell tests, comprising of normal cells, squamous carcinoma, furthermore, adenocarcinoma cells. The trial comes about show that the optical polarimetry might be demonstrated amazingly helpful in separating among sound and lung cancer cells too as separating among various lung cancer cells.

REFERENCES

[1] **World Health Organization, Cancer. [Online]. Available:http://www.who.int/mediacentre/factsheets/fs297/en/, accessedNov. 30, 2014.**

[2] **N. Hollings and P. Shaw, "Diagnostic imaging of lung cancer," Eur.Respirat. J., vol. 19, no. 4, pp. 722–742, Apr. 2002.**

[3] **D. R. Aberle et al., "Reduced lung-cancer mortality with low-dose computed tomographic screening," New England J. Med., vol. 365, no. 5, pp. 395–409, 2011.**

[4] **L. Hutchinson, "Screening: Improved model for lung cancer detection,"Nature Rev. Clin. Oncol., vol. 10, no. 4, p. 183, Apr. 2013.**

[5] **G. C. Giakos et al., "Stokes parameter imaging of multi-index of refraction biological phantoms utilizing optically active molecular contrast agents," Meas. Sci. Technol., vol. 20, no. 10, p. 104003, 2009.**

[6] **C. Balas, "Review of biomedical optical imaging—A powerful, noninvasive,non-ionizing technology for improving in vivo diagnosis," Meas. Sci. Technol., vol. 20, no. 10, p. 104020, 2009.**

[7] **G. C. Giakos et al., "Polarimetric phenomenology of photons with lung cancer tissue," Meas. Sci. Technol., vol. 22, no. 11, p. 114018, 2011.**

[8] **G. C. Giakos et al., "Near infrared light interaction with lung cancer cells," in Proc. IEEE Instrum. Meas. Technol. Conf. (I2MTC), May 2011, pp. 1–6.**

[9] **K.-C. Huang, C.-L. Chang, and W.-H. Wu, "Novel image polarization method for measurement of lens decentration," IEEE Trans. Instrum. Meas., vol. 60, no. 5, pp. 1845–1853, May 2011.**

[10] **S. Liao et al., "Passive millimeter-wave dual-polarization imagers," IEEE Trans. Instrum. Meas., vol. 61, no. 7, pp. 2042–2050, Jul. 2012.**

[11] **G. C. Giakos, "Novel biological metamaterials, nanoscale optical devices, and polarimetric exploratory data analysis (pEDA)," Int. J.**

[12] **Signal Imag. Syst. Eng., vol. 3, no. 1, pp. 3–12, 2010.**

[13] **G. C. Giakos et al., "Infrared photon discrimination of lung cancer cells," in Proc. IEEE Int. Conf. Imag. Syst. Techn. (IST), Jul. 2012, pp. 637–642.**